Identification of charge states of indium vacancies in InP using the positron-electron auto-correlation function

1998 J. Phys.: Condens. Matter 10 9263

(http://iopscience.iop.org/0953-8984/10/41/008)

J. Phys.: Condens. Matter **10** (1998) 9263–9271. Printed in the UK PII: S0953-8984(98)95760-5

Identification of charge states of indium vacancies in InP using the positron–electron auto-correlation function

W LiMing†, S Fung†, C D Beling†, M Fuchs‡ and A P Seitsonen‡

† Department of Physics, The University of Hong Kong, Pokfulam Road, Hong Kong, People's Republic of China

‡ Fritz-Haber-Institut, der Max-Planck-Gesellschaft, Faradayweg 4-6, 14195 Berlin-Dahlem, Germany

Received 9 July 1998

Abstract. The positron–electron auto-correlation function (ACF) is calculated for neutral and negatively charged indium vacancies in InP as well as a perfect InP material. *Ab initio* calculations are performed for the electron wave functions in the density functional theory (DFT) with the local density approximation (LDA) for the exchange–correlation potential of electrons. The positron wave function is calculated by directly diagonalizing the single-particle Hamiltonian of the positron in the LDA with a density-gradient correction. It is found that the ACF is suitable for identifying the charge states of the indium vacancies. Neutral indium vacancies greatly diminish the nearest peaks and dips (P1 and D1) of the ACF which are located after the nearest-neighbouring lattice points in the case of a perfect material. Negatively charged indium vacancies nearly eliminate these peaks and dips, together with the next-nearest peaks (P2) located at the next-nearest-neighbouring lattice points. Therefore, the diminution of the P1 and D1 can be taken as an indication of the formation of neutral indium vacancies, and that of the P2 can be taken as an indication of the formation of negatively charged indium vacancies. However, the three negative charge states of the indium vacancies (V_{In}^{1-}, V_{In}^{2-} and V_{In}^{3-}) are still difficult to distinguish from each other by means of the ACF method.

1. Introduction

Point defects in semiconductors are of great importance to the electronic and optical properties of semiconductors. Firstly, they are closely related to the unreliability and degradation of the electronic or optical devices. Secondly, they may work in a beneficial way in some semiconductor devices. Point defects can acts as donors, acceptors, carrier traps or scattering or recombination centres, causing shallow or deep levels in the energy gaps of semiconductors. A point defect can be electrically active, resulting in different charge states: positive, neutral or negative, to compensate the dangling bonds at the point defect. However, the identification of the point defects in materials has proved to be difficult.

The positron annihilation technique has proved to be a powerful tool to detect point defects in materials. This is because positrons can be trapped by point defects, where the chemical environment is very different from that in the bulk, thus giving different positron lifetimes and some other characteristics. Accordingly, a great number of studies on different types of point defect have been carried out using the positron annihilation technique in the past decades [1–3]. Many studies are stimulated by the observation of the deep level EL2 in GaAs, which is believed to be caused by the As antisites [4]. An interesting observation is that positrons are much more sensitive to negatively charged states of point defects since

0953-8984/98/419263+09$19.50

this type of defect is more attractive to positrons. When a transition between different charge states takes place the point defects may change their positron trapping rates and hence the average positron lifetimes in them. This effect has been observed by Corbel and colleagues, who found a transition from V_{As}^{-} to V_{As}^{0} in n-GaAs by measuring the positron lifetime (257 ps to 295 ps) at different temperatures [5, 6]. They also found that this transition corresponds to a narrower momentum distribution (MD) from their measurements of two-dimensional angular correlation of annihilation radiation (2D-ACAR). Therefore, the positron annihilation technique provides fingerprints for the charge states of the point defects in materials.

There is growing interest in the characterization of the properties of defects in the III–V compound semiconductor InP [7–10]. The undoped LEC-grown InP material is n-type. It was reported that this material can be compensated to be semi-insulating by means of annealing at 800–900 °C for about 90 hours. As pointed out by Zhao *et al* [10], there may exist many types of point defect in this material, including indium vacancies (V_{In}), phosphorus vacancies (V_P), hydrogen-complex vacancies ($V_{In}H_4$), phosphorus antisites (In_P) and indium antisites (P_{In}). Furthermore, these vacancies may have different charge states. According to the calculations of Seitsonen *et al* [11], all charge states of indium vacancies are located in the lower half of the gap, and most other point defects are located in the upper half of the band gap. Indeed, Polity and Engelbrecht had found a few negative charge states in their electron-irradiated InP samples after annealing at 430–590 K [7].

It is well known that positrons trapped in vacancies mainly annihilate with the valence electrons, giving stronger low momentum annihilation compared to annihilation in the bulk. Recently, Hakala *et al* have calculated the MD in the vacancy clusters in Si[12]. They found a systematic narrowing of the MD spectra as the size of the vacancy increases. In this work, however, not the MD but the positron–electron auto-correlation function (ACF), which is the Fourier transformation of the MD spectrum, is calculated. This is because the low momentum information in the MD can be reflected more clearly in the higher positions of the ACF, especially in the case of defects. Generally speaking, the ACF oscillates and attenuates on the lattice of the crystal up to a distance of about 12 Å. The nodes of the ACF take the lattice positions with a slight outward shift. The oscillation of the ACF reflects the periodicity of the crystal. The distortion of the periodicity can lead to the disappearance of the oscillation of the ACF. The ACF looks like the diffraction pattern in the x-ray diffraction measurements.

In the present work an *ab initio* calculation based on the density functional theory (DFT) in the local density approximation (LDA), as described by Seitsonen *et al* [11], has been performed to determine the electron wave functions and densities in various charge states of the indium vacancies in InP. We use a 54-atom supercell with the zinc-blende structure with an indium vacancy (53 atoms). Norm-conserving separable pseudopotentials of the Hamann type are used in the separable form of Kleinman and Bylander [13, 14]. A plane-wave basis is used to expand the wave functions, with an energy cut-off of 8 Ryd. The Brillouin zone is sampled with the Monkhorst–Pack $2 \times 2 \times 2$ $\boldsymbol{k}$ point mesh (two special $\boldsymbol{k}$ points). It is believed that the positron does not affect the electronic states significantly due to the screening effect of the electron cloud around the positron [12] although the positron may affect the atomic relaxation of the vacancies. The positron wave function is calculated by means of directly diagonalizing the single-particle Hamiltonian. The potential sensed by the positron contains the Coulomb potentials from the ions and valence electrons and the correlation potential between the positron and the electrons [16]. A density-gradient correction to the positron annihilation has been included [17]. A brief introduction of the formalism of the theory is given in section 2. Results and discussion are given in section 3.

2. Theory

The positron–electron ACF is defined by [18]

$$B^{2\gamma}(\boldsymbol{r}) = \sum_i \int_V \psi_i^{ep}(\boldsymbol{s})^* \psi_i^{ep}(\boldsymbol{r}+\boldsymbol{s}) \mathrm{d}^3 s \tag{1}$$

where $\psi_i^{ep}(\boldsymbol{r})$ is the two-particle wave function of the positron–electron pair, and V is the volume of the crystal. This wave function can be approximated using the single-particle wave functions, $\psi_+(\boldsymbol{r})$ and $\psi_{n\boldsymbol{k}}(\boldsymbol{r})$, of the positron and electron, respectively, and taking into account the enhancement effect of the positron annihilation [19]:

$$\psi_i^{ep}(\boldsymbol{r}) = \psi_+(\boldsymbol{r})\psi_{n\boldsymbol{k}}(\boldsymbol{r})\sqrt{\gamma_{n\boldsymbol{k}}(\boldsymbol{r})} \tag{2}$$

where n is the electron band index, $\boldsymbol{k}$ is the wave vector, and $\gamma_{n\boldsymbol{k}}(\boldsymbol{r})$ is the enhancement factor. Since we are interested in positron annihilation in vacancies, which happens mainly between a positron and a valence electron, the summation in equation (1) can be taken over the wave vectors in the Brillouin zone and the occupied valence electron bands. At finite temperature the Fermi–Dirac distribution of the electrons should be included in the summation in equation (1). To solve the electron and positron wave functions we use a plane wave basis to expand the wave functions:

$$\psi_{n\boldsymbol{k}}(\boldsymbol{r}) = \frac{1}{\Omega}\sum_{\boldsymbol{G}} C_{n\boldsymbol{k}}(\boldsymbol{G}) \exp[\mathrm{i}(\boldsymbol{G}+\boldsymbol{k})\cdot\boldsymbol{r}] \tag{3}$$

$$\psi_+(\boldsymbol{r}) = \frac{1}{V}\sum_{\boldsymbol{G}} D(\boldsymbol{G}) \exp(\mathrm{i}\boldsymbol{G}\cdot\boldsymbol{r}) \tag{4}$$

where $\boldsymbol{G}$ are the reciprocal lattice vectors, and Ω is the unit cell volume. The positron occupies the Γ point in the Brillouin zone when the temperature is not very high, because in general only one positron is involved at any time.

The electron wave functions are solved using the Car–Parrinello *ab initio* method based on the DFT in the LDA for the exchange and correlation [11]. The computer program package `fhi96md` is employed [20]. The Verlet algorithm is used to relax the atomic system. The pseudo-potentials are constructed following the scheme of Bachelet *et al* [13] in the fully separable Kleinman–Bylander form [14, 15]. The energy cutoff is 8 Ryd, which requires about 3500 plane waves in the summations of equations (3) and (4). The lattice constant of InP is 5.87 Å. A 54-atom supercell is used to model the indium vacancy (53 atoms) in the zinc-blende structure. The Brillouin zone is sampled by two special $\boldsymbol{k}$ points $(2\pi/a)(1/4, 1/4, 1/4)$ and $(2\pi/a)(3/4, 3/4, -1/4)$. The initialization of the wave functions is carried out by an expansion in the pseudo-atomic orbitals. For the charged indium vacancies a rigid background charge density is introduced in order to neutralize the supercell. It has been assumed that the positron even in a vacancy does not affect the electron states significantly as pointed out by Hakala *et al* [12]. The positron wave function is solved by directly diagonalizing the single-positron Hamiltonian in the plane wave basis. The potential of the positron contains the point-core ionic potential, the electron Hartree potential and the correlation potential of Boronski and Nieminen [16]. The density-gradient correction of Barbiellini *et al* [17] has been taken into account in the correlation potential and the enhancement factor.

The enhancement factor can be approximated as an average in the Brillouin zone, becoming a density-dependent-only (thus a periodic) function, $\gamma(n_-(\boldsymbol{r}))$ [17]. Since the

positron wave function is also a periodic function we can expand the enhancement factor and the positron wave function together in the plane wave basis:

$$\psi_+(\boldsymbol{r})\sqrt{\gamma(n_-(\boldsymbol{r}))} = \frac{1}{V}\sum_{\boldsymbol{G}} D_{enh}(\boldsymbol{G})\exp(\mathrm{i}\boldsymbol{G}\cdot\boldsymbol{r}). \tag{5}$$

Finally, using the expansions (3) and (5) the ACF can be written as

$$B^{2\gamma}(\boldsymbol{r}) = \frac{1}{V}\sum_{\boldsymbol{k}}\exp(\mathrm{i}\boldsymbol{k}\cdot\boldsymbol{r})\sum_{G}\exp(\mathrm{i}\boldsymbol{G}\cdot\boldsymbol{r})\sum_{n} f_n(\boldsymbol{k})|\sum_{\boldsymbol{G}_1} D_{enh}(\boldsymbol{G}_1)C_{n\boldsymbol{k}}(\boldsymbol{G}-\boldsymbol{G}_1)|^2 \tag{6}$$

where $f_n(\boldsymbol{k})$ is the Fermi–Dirac distribution function, and the $\boldsymbol{k}$ summation is taken using the Chadi–Cohen scheme [21].

This formalism also provides a method for calculating the MD of positron annihilation radiation, i.e., one obtains simply the MD from the Fourier transformation of the ACF.

As a test for the positron and electron wave functions we also calculate the positron lifetimes in a perfect InP material and in different charge states of indium vacancies. Positron lifetime is the inverse of positron annihilation rate, which is given by [17]

$$\lambda = \pi r_0^2 c\int n_+(\boldsymbol{r})n_-(\boldsymbol{r})\gamma(n_-(\boldsymbol{r}))\mathrm{d}^3r \tag{7}$$

where $n_+(\boldsymbol{r})$ and $n_-(\boldsymbol{r})$ are the positron and electron densities, respectively.

3. Results and discussion

First, we report the positron lifetimes in a perfect InP material, and in InP materials with neutral indium vacancies and negatively charged indium vacancies, as listed in table 1. The lifetime (241.5 ps) in a perfect InP material is close to the experimental value (240.6 ps) measured by Polity and Engelbrecht [7]. The lifetime (313.5 ps) for the neutral indium vacancies is much larger than that calculated by Alatalo *et al* (280 ps). Polity and Engelbrecht found a component of 310 ps in their electron irradiated InP materials after annealing at 430–590 K. This component was attributed to divacancies, because it is much larger than the value of Alatalo *et al* for indium mono-vacancies. This may not be the case. We found that the calculation of positron lifetimes is very sensitive to the atomic relaxation of the vacancies. An incomplete relaxation will lead to lower positron lifetime, e.g., the calculated lifetime is only 248 ps in neutral indium vacancies without relaxation. Therefore, we prefer to assign the 310 ps component of Polity and Engelbrecht to the positron lifetime in neutral indium vacancies. Indeed, they have observed a strong temperature dependence of this component, which suggests a transition of the indium vacancies between different charge states. The point is that there is a clear tendency that the positron lifetime decreases with increasing negative charge of the indium vacancy.

Table 1. Positron lifetimes (in ps) in a perfect InP material, and in indium vacancies with different charge states.

	Perfect InP	V_{In}^{0}	V_{In}^{1-}	V_{In}^{2-}	V_{In}^{3-}
Present work	241.5	313.5	303.2	272.9	262.0
Experiment [a]	240.6	310±15	—	—	—

[a] The result measured Polity and Engelbrecht [7]. The 310 ps component is explained as the lifetime in divacancies.

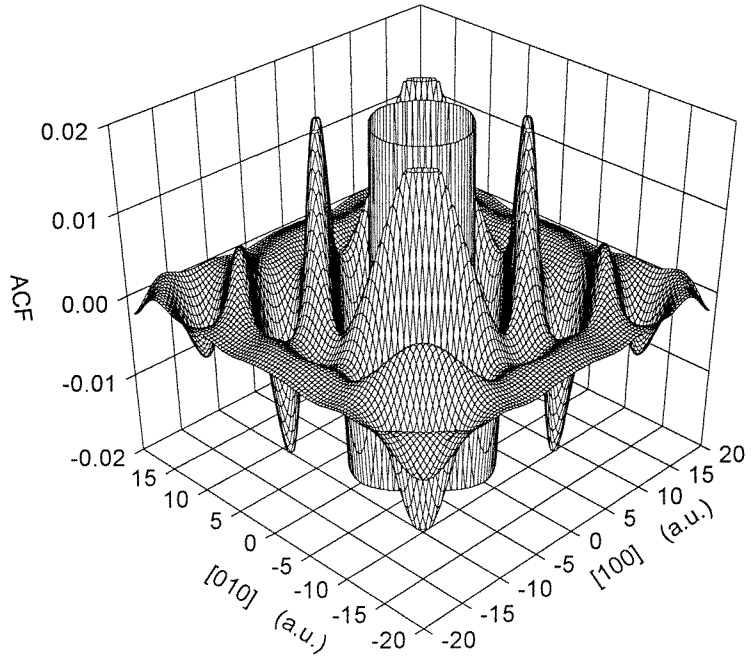

(a)

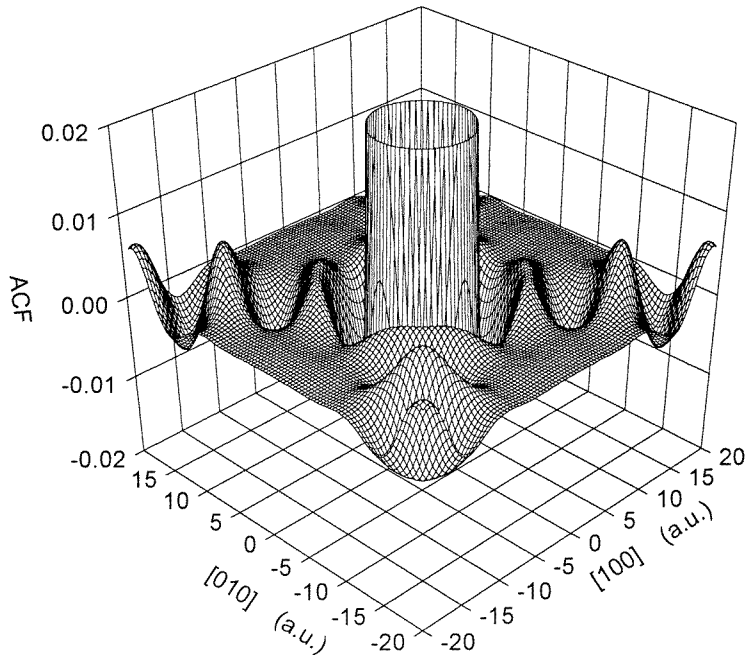

(b)

Figure 1. Auto-correlation function (a) in a perfect InP material and (b) in InP with neutral vacancies. The value of the central peak has been normalized to unity. To show the detailed structure the peak has been cut at 0.02.

Now we show the ACFs, on the plane of (001), of positron annihilation radiation in a perfect crystal and in various negatively charged indium vacancies. In all the figures the peak values of the ACF have been normalized to unity and the central peaks have been cut at 0.02 for clarity. The ACF in a perfect lattice of InP is shown in figure 1(a). There are strong oscillations in the equivalent ⟨110⟩ directions. This reflects the strong anisotropy of the electron wave functions in the crystal due to the atomic bonding in these directions. The nodes of the ACF on the rising slopes of the peaks pass nearly through the lattice points in these directions. In this sense the ACF looks like a pattern of the lattice points as in the case of x-ray diffraction. As pointed out by the present authors earlier [22], these nodes shift outwards slightly from the lattice points because of the introduction of the positron wave function. The nodes of the ACF of the perfect InP read 8.16, 15.96 and 24.01 a.u., corresponding to the lattice points 7.84, 15.68 and 23.52 a.u. in the [110] direction. If the positron wave function is set to be unity, the nodes will coincides with the lattice points exactly. This is the case in the Compton profile measurements. Outside the central peak are the four peaks and four dips following the nearest-neighbouring lattice points. These peaks and dips have a height of about 2% of that of the central peak. One will see that these peaks and dips are sensitive to vacancies and their charge states. Let these nearest peaks and dips be denoted as P1 and D1, respectively. The peaks and dips following the next-nearest neighbouring lattice points can also be seen clearly, thus being denoted as P2 and D2.

Figure 1(b) shows the ACF in an InP crystal with neutral indium vacancies. It can be seen that the P1 and D1 significantly attenuate, to heights of 10% and 25% of those of the perfect crystal, respectively. However, the P2 and D2 have hardly changed their heights. This means that the neutral vacancy greatly diminishes the P1 and D1 only. This becomes an indication of the formation of vacancies. Another important effect is that the ACF pattern spreads outwards compared to that in the perfect InP crystal. This is because the momentum of the positron annihilation radiation is lowered since the positrons are localized in the vacancies and thus annihilate much more readily with the valence electrons. For the negatively charged vacancies the atoms around the vacancies are more relaxed inwards and the positrons are more localized in the vacancies. The ACFs of positron annihilation in V_{In}^{1-} and V_{In}^{3-} are shown in figures 2(a) and (b). It is seen that the P1 and D1 nearly disappear. More importantly, the P2 also nearly disappear. However, the D2 remains nearly unchanged. Therefore, the negative charge of the indium vacancy depresses mainly the P2. One obtains another indication for the formation of the charged vacancies. Because the P2 and D2 are weak compared to the central peak they will be invisible in their Fourier transforms, i.e., the 2D-ACAR spectra or the Doppler-Broadening spectra. Therefore, people generally see only a narrowing of the Gaussian-like spectrum with increasing charges of the vacancies.

Nevertheless, to identify the different charge states V_{In}^{1-} , V_{In}^{2-} and V_{In}^{3-} is still difficult. Figures 2(a) and (b) show that the ACFs for the V_{In}^{1-} and V_{In}^{3-} are difficult to distinguish from each other. However, the ACFs of these charge states are distinctly different from that of the neutral state as shown in figure 1(b). The neutral vacancies greatly diminish the P1 and D1, while keeping the P2 and D2 unchanged. However, the charged vacancies virtually eliminate not only the P1 and D1 but also P2 while keeping the D2 unchanged. This makes it possible to identify the charged vacancies and the neutral vacancies by observing the disappearance of P1, D1 and P2.

To see the characteristics of the ACF in these different charge states of indium vacancies more clearly we plot the ACFs in the perfect InP, V_{In}^{1-} , V_{In}^{2-} and V_{In}^{3-} in the [110] direction in figure 3. The P1 and D1 of the ACF first fall in the neutral vacancy, and the ACF spreads outwards. Then the P2 falls in the charged indium vacancies and the P1 and D1

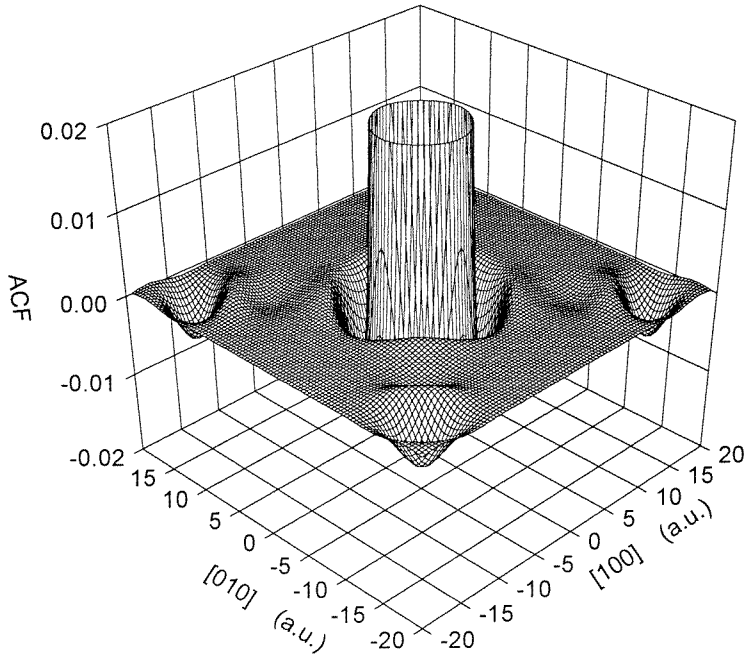

(a)

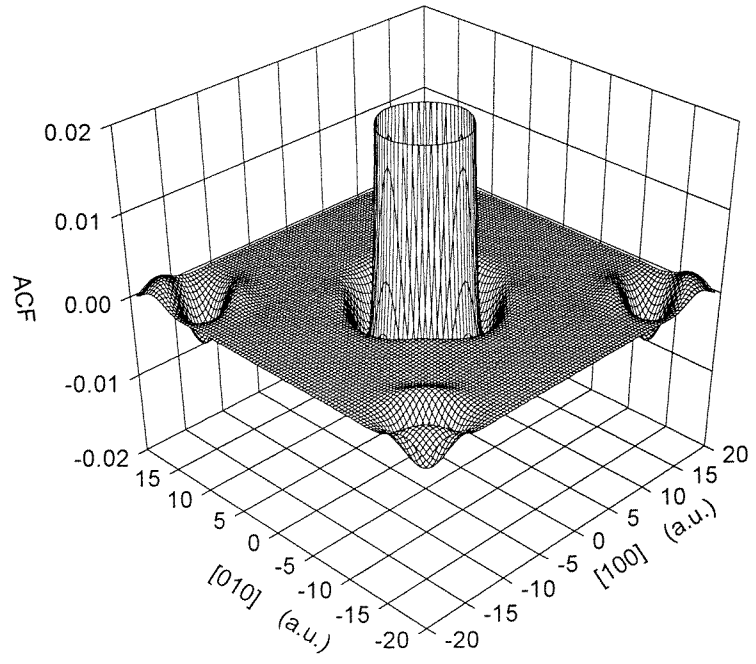

(b)

Figure 2. Auto-correlation function in InP with (a) V_{In}^{1-} and (b) V_{In}^{3-} vacancies. The value of the central peak has been normalized to unity. To show the detailed structure the peak has been cut at 0.02.

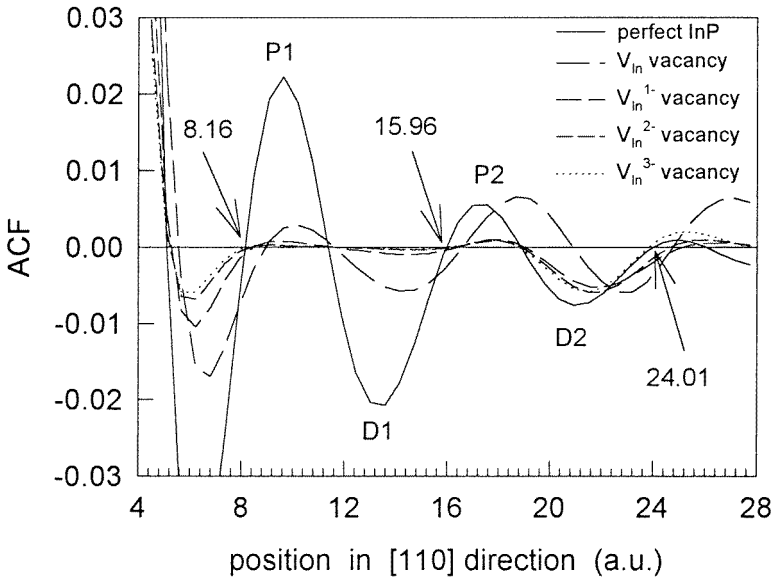

Figure 3. Auto-correlation function in the [110] direction in perfect InP and in indium vacancies with different charge states. The nodes of the auto-correlation function in perfect InP correspond to the lattice positions in the [110] direction with an outward shift. The arrows are guides of the nodes for the eyes. P1 and D1 denote the nearest peaks and dips, respectively; P2 and D2 denote the next-nearest peaks and dips, respectively.

nearly disappear. It can also be seen that, with increasing charge of the indium vacancies, the ACF contracts, resulting from the atomic relaxation of the charged vacancies.

In summary, the auto-correlation function method provides a tool to identify the charged vacancies and neutral vacancies. In the case of the InP material, the nearest peaks and dips of the ACF are firstly diminished by the neutral indium vacancies and then nearly disappear in the charged indium vacancies. The next-nearest peaks are nearly eliminated in the charged indium vacancies. However, the next-nearest dips are kept nearly unchanged in various charge states. The diminution and elimination of these peaks and dips can be taken as indications of the formation of neutral and charged indium vacancies.

Acknowledgments

S Fung wishes to acknowledge valuable financial support from the HKU CRCG and the Hong Kong RGC research grants.

References

[1] Kuisma S, Saarinen K, Hautojarvi P and Corbel C 1996 *Phys. Rev.* B **53** R7588
[2] Corbel C, Pierre F, Saarinen K and Hautojarvi P 1992 *Phys. Rev.* B **45** 3386
[3] Dannefaer S, Mascher P and Kerr D 1989 *J. Phys.: Condens. Matter* **1** 3213
[4] Saarinen K, Kuisma S, Hautojarvi P, Corbel C and LeBerre C 1994 *Phys. Rev.* B **49** 8005
[5] Corbel C, Leberre C, Saarinen K and Hautojarvi P 1997 *Mater. Sci. Eng.* **B4** 173
[6] Ambigapathy R, Manuel A A, Hautojarvi P, Saarinen K and Corbel C 1994 *Phys. Rev.* B **50** 2188
[7] Polity A and Engelbrecht T 1997 *Phys. Rev.* B **55** 10480
[8] Ewels C P, Oberg S, Jones R, Pajot B and Briddon P R 1996 *Semicond. Sci. Technol.* **11** 502

[9] Carnera A, Gasparotto A, Tromby M, Caldironi M, Pellegrino S, Vidimari F, Bocchi C and Frigeri C 1994 *J. Appl. Phys.* **76** 9
[10] Zhao Y W, Xu X L, Gong M, Fung S and Beling C D 1998 *Appl. Phys. Lett.* **72** 2126
[11] Seitsonen A P, Virkkunen R, Puska M J and Nieminen R M 1994 *Phys. Rev.* B **49** 5253
[12] Hakala M, Puska M J and Nieminen R M 1998 *Phys. Rev.* B **57** 7621
[13] Bachelet B B, Hamann D R and Schluter M 1982 *Phys. Rev.* B **26** 4199
[14] Kleinman L and Bylander D M 1982 *Phys. Rev. Lett.* **48** 1425
[15] Fuchs M, Bockstedte M and Scheffler M 1998 private communication
[16] Boronski E and Nieminen R M 1986 *Phys. Rev.* B **34** 3820
[17] Barbiellini B, Puska M J, Korhonen T, Harju A, Torsti T and Nieminen R M 1996 *Phys. Rev.* B **53** 16201
[18] Kobayasi T 1994 *Bull. Coll. Med. Sci.* Tohoku University 3(1) 11
[19] Alatalo M, Kauppinen H, Saarinen K, Puska M J, Makinen J, Hautojarvi P and Nieminen R M 1995 *Phys. Rev.* B **51** 4176
[20] Bockstedte M, Kley A, Neugabauer J and Scheffler M 1997 *Commut. Phys. Commun.* **10** 187
[21] Chadi D J and Cohen M L 1973 *Phys. Rev.* B **7** 692
[22] LiMing W, Panda B K, Fung S and Beling C D 1997 *J. Phys.: Condens. Matter* **9** 8147